

## Change and asymmetry of magnetization reversal for a Co/CoO exchange-bias system

M. Gierlings,<sup>1</sup> M. J. Prandolini,<sup>2</sup> H. Fritzsche,<sup>1</sup> M. Gruyters,<sup>1</sup> and D. Riegel<sup>1</sup>

<sup>1</sup>Hahn-Meitner-Institut Berlin, Glienicker Strasse 100, 14109 Berlin, Germany

<sup>2</sup>Institut für Experimentalphysik (WE1), Freie Universität Berlin, 14195 Berlin, Germany

(Received 15 October 2001; published 11 February 2002)

A drastic change of magnetization reversal processes in [Co/CoO/Au]<sub>20</sub> multilayers has been found by polarized neutron reflectometry. For the unbiased state ( $T=300$  K), reversal is due to rotation on both sides of the hysteresis loop. In the exchange-bias state ( $T=10$  K), rotation is the main mechanism only for increasing fields. For the decreasing field branch, which is in the direction opposite to the bias (cooling field), the mechanism changes to domain-wall motion. A major advantage of the present CoO/Co system is the independence of exchange bias on cooling field orientation.

DOI: 10.1103/PhysRevB.65.092407

PACS number(s): 75.70.Ak, 75.30.Gw, 75.70.Cn

A characteristic shift of the magnetic hysteresis loop away from zero field has initially been found in ferromagnetic (FM) Co particles having an antiferromagnetic (AFM) CoO coating.<sup>1</sup> This phenomenon, which has been called exchange bias (EB), is often observed after field cooling FM/AFM systems below the Néel temperature  $T_N$ . In the past two decades, EB has intensively been studied in thin films<sup>2</sup> where it has a high potential for technological applications. In at least some EB systems different reversals for the increasing and decreasing field branch can readily be identified by the shape of the hysteresis loop,<sup>3-7</sup> and it is well established now that reversal asymmetry is of crucial importance to elucidate unidirectional behavior in this large group of magnetic systems.<sup>8-12</sup>

Magnetization curves belong to the fundamental macroscopic properties characterizing ferromagnetic materials. The specific type of reversal is determined by various subtle contributions such as exchange interaction or magnetic anisotropy. Magnetization can be reversed either by rotation or domain-wall (DW) motion. For single thin layers, nucleation and DW motion are the dominant mechanisms because they are energetically more favorable. For granular soft magnetic materials, the relevant mechanism can strongly depend on the direction of magnetocrystalline anisotropy<sup>13</sup> or material composition.<sup>14</sup> For double layers such as AFM/FM systems, reversal may drastically change due to the coupling at the interface. Recent investigations have shown that depending on the particular system, both DW motion and rotation can be preferred.<sup>8-12,15,16</sup> In this work, a polarized neutron reflectometry (PNR) study on a [Co/CoO/Au]<sub>20</sub> multilayer exhibiting EB of strong unidirectional anisotropy is presented. Because PNR provides a ready means to measure not only the in-plane magnetization parallel but also perpendicular to the external field, we are able to elucidate the mechanisms responsible for asymmetry of the magnetization curve.

Two samples of a [Co(16.4 nm)/CoO(2 nm)/Au(3.4 nm)]<sub>20</sub> multilayer were prepared simultaneously on Al<sub>2</sub>O<sub>3</sub>(0001) substrates (thickness: 1 mm): one of a large film area of 15×30 mm<sup>2</sup> and another of a small film area of ≈16 mm<sup>2</sup>. CoO/Co bilayers are separated by Au spacer layers to avoid magnetic interaction between neighboring exchange-biased AFM/FM pairs. Co and Au were grown by molecular-beam epitaxy at a low rate of 0.1–0.2 nm/min at a

base pressure of the ultrahigh-vacuum chamber of 10<sup>-10</sup> mbar and a growth temperature of 300 K. Purity of substrate and layers was checked by Auger electron spectroscopy while x-ray measurements revealed a single crystalline fcc(111) surface orientation of Co. CoO layers of 2 nm thickness were obtained by an *in situ* oxidation method using a controlled exposure of high-purity oxygen gas.<sup>7,17</sup> Magnetic properties of the multilayer were characterized by magnetometry (small sample) using a superconducting quantum interference device and by PNR (large sample). PNR experiments were performed with the standard setup of the reflectometer V6 at the Hahn-Meitner-Institut Berlin with a neutron wavelength  $\lambda=4.66$  Å.<sup>18</sup>  $\Theta-2\Theta$  specular reflectivity scans with a normal wave vector  $|Q|=4\pi\sin\Theta/\lambda$  were recorded for all four cross sections: (+ +), (– –), (+ –), and (– +). The sign +(–) denotes the neutron polarization state parallel (antiparallel) with respect to applied fields in front of (behind) the sample. The first (second) sign refers to the state before (after) reflection from the sample. The two non-spin-flip (NSF) cross sections, (+ +) and (– –), yield information on the nuclear structure and the in-plane magnetization of the sample parallel to the external field axis. For the two spin-flip (SF) cross sections, (+ –) and (– +), the neutron polarization is changed due to interaction with the sample. These intensities are exclusively of magnetic origin and correspond to the in-plane magnetization perpendicular to the external field.

A magnetization curve has been recorded at  $T=10$  K (Fig. 1) after cooling in a field  $H_{cool}=+4000$  Oe from above  $T_N=293$  K of bulk CoO. A hysteresis loop measurement, performed at 300 K, shows no shift and has small coercivities  $H_C$  of less than 20 Oe. This is typical for thin films with soft magnetic properties.<sup>7,17</sup> At  $T=300$  K, which is sufficiently above the blocking temperature  $T_B=180$  K for EB in this particular type of CoO/Co system, there is virtually no magnetic coupling between CoO and Co (unbiased state).<sup>17</sup> On the other hand, in the biased state ( $T=10$  K) the hysteresis loop is considerably shifted away from zero field (EB field  $H_E=-393$  Oe) featuring different coercivities  $H_{ca}=-895$  Oe (antiparallel  $H_{cool}$ ) and  $H_{cp}=+110$  Oe (parallel  $H_{cool}$ ) for decreasing and increasing fields, respectively. A close inspection of the loop shape provides the first information on the underlying reversal mecha-

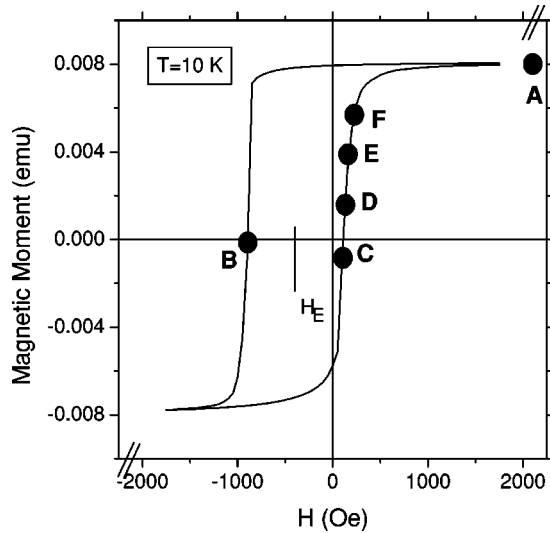


FIG. 1. Magnetic hysteresis loop for the biased state at  $T = 10$  K (after cooling in a field  $H_{cool} = +4000$  Oe from  $T = 300$  K).

nisms: For decreasing fields, magnetization remains in saturation up to a high coercive field  $H_{ca}$  before a sudden reversal takes place. On the opposite side, the return to saturation for increasing fields leads to a rounded edge of the hysteresis loop. The observed behavior is even more pronounced in the corresponding simple CoO/Co bilayers.<sup>7,17</sup> Using the product of the EB field  $H_E$ , the Co magnetization and the Co thickness as a measure of the interfacial energy  $E_{int}$  a value of  $0.9$  erg/cm<sup>2</sup> ( $T = 10$  K) is obtained.<sup>7,17</sup> Another important measure of the unidirectional character is the  $H_E/H_C$  ratio ( $H_C$  being the half width of the hysteresis loop) which amounts to as much as  $0.78$ .

Neutron reflectivity profiles corresponding to three characteristic fields in the magnetization curve of the biased state are shown in Fig. 2. These field values have also been marked by circles in Fig. 1. Solid lines are fits to the NSF reflectivity using a simulation program which is based on the Parratt formalism.<sup>19</sup> We focus on the reflectivity profiles within a small range of wave vector  $Q$  featuring only one characteristic peak. In this range, peak positions for  $(++)$  and  $(--)$  reflection profiles can considerably differ depending on different magnetic contributions to the neutron potential. For magnetic saturation [Fig. 2(a)], each of the two NSF reflectivity profiles is characterized by only one dominant peak. These peaks are clearly separated from each other. Apart from a background of less than  $10^{-3}$ , there is no significant contribution in the SF profiles, which is expected for the sample magnetization completely aligned with the external field.

For  $H \approx H_{ca}$  [Fig. 2(b)], both NSF profiles now clearly exhibit two peaks at the same positions as observed in Fig. 2(a). Obviously, the sample magnetization now mainly consists of domains pointing either parallel or antiparallel to the applied field. That is, almost identical cross sections for  $(++)$  and  $(--)$  neutrons correspond to an almost equal distribution of domains with parallel or antiparallel magnetization. This behavior is further illustrated by the curve fit

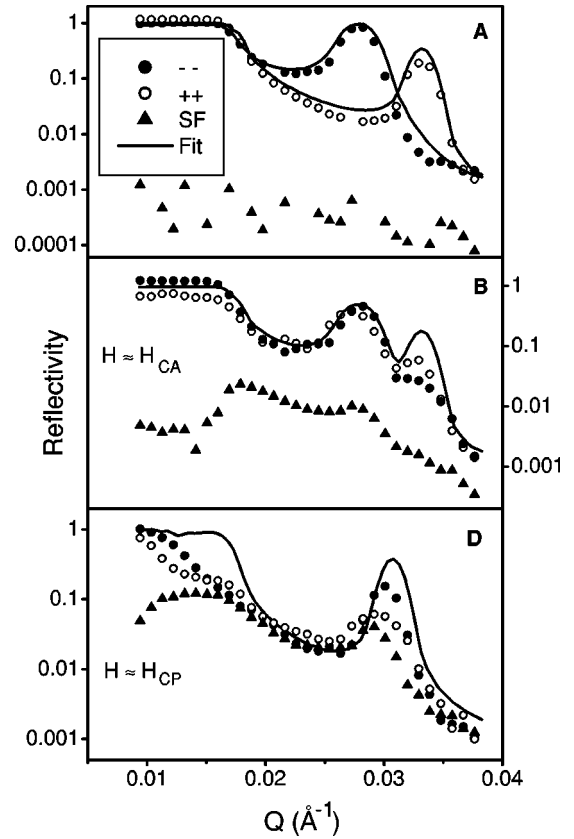


FIG. 2. Polarized neutron reflectivity (PNR) profiles corresponding to three characteristic fields in the hysteresis loop in the biased state [marked by circles in Fig. 1(a); magnetic saturation, (b) coercivity at decreasing fields  $H \approx H_{ca}$ , and (d) coercivity at increasing fields  $H \approx H_{cp}$ ].

which represents an intuitive model simply adding half of the calculated intensity of the  $(++)$  and  $(--)$  profiles of the saturated state [Fig. 2(a)]. The model does not account for SF processes and diffuse scattering from domain walls. The resulting net magnetization of the observed domain configuration is zero. The corresponding SF profile in Fig. 2(b) indicates a small amount of magnetization perpendicular to the applied field. But, a reflectivity of only  $10^{-2}$  implies that either the degree of rotation is minimal or only a small part of the total multilayer magnetization has been rotated. It can therefore be concluded that the observed configuration with magnetization pointing either parallel or antiparallel to the applied field originates from a reversal which is mainly due to DW motion. This is further supported by additional reflectivity profiles (not shown here) on the decreasing field branch with external fields slightly higher or lower than  $H = -883$  Oe  $\approx H_{ca}$  of Fig. 2(b). The latter also reveals two peaks with fixed positions but with varying intensities according to an increasing or decreasing amount of domains with either parallel or antiparallel magnetization.

Close to the opposite coercivity  $H_{cp}$  [Fig. 2(d)], both NSF profiles clearly show only one dominant peak at a changed position [which is between the peak positions in Fig. 2(a) and Fig. 2(b)]. This position is very close to the peak found by the simulation when only the nuclear contributions to the

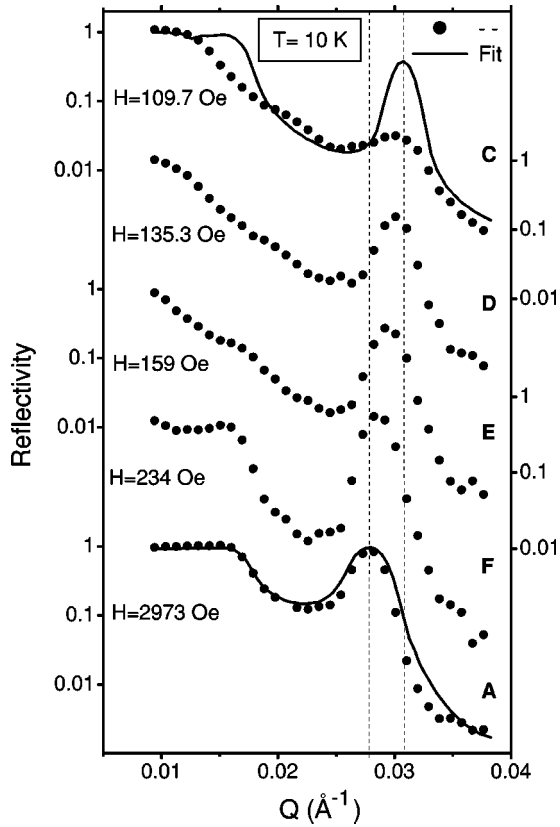


FIG. 3. Non-spin-flip profiles (—) for different magnetic fields (marked by circles in Fig. 1) in the increasing field branch of the hysteresis loop for the biased state ( $T=10$  K).

neutron potential are included [solid line in Fig. 2(d)]. Additionally, the reflectivity in the SF profile is of the same magnitude as in the NSF profiles. This unambiguously proves that the main part of the magnetization has been rotated in the plane of the sample perpendicular to the external field. Contrary to the behavior found for  $H \approx H_{ca}$ , the reversal mechanism in the increasing field branch ( $H \approx H_{cp}$ ) is obviously due to rotation. However, it should be mentioned that a certain amount of off-specular reflection has also been recorded by a position sensitive detector. Spin-dependent diffuse scattering can be considerable in EB systems.<sup>20</sup> However, this effect does not change the conclusions on the magnetization processes given above.

Two sets of NSF reflectivity profiles at different fields (for the low-temperature measurement marked by circles in Fig. 1) in the increasing field branch of the magnetization curve are shown in Figs. 3 and 4 for the biased state ( $T=10$  K) and the unbiased state ( $T=300$  K), respectively. Close to the coercive fields ( $H = +110$  Oe at  $T=10$  K and  $H = +6.5$  Oe at  $T=300$  K), NSF profiles reveal one dominant peak at a position corresponding only to the nuclear contributions of the neutron potential. With increasing fields this peak shifts towards the position corresponding to the maximum magnetic contribution to the neutron potential [i.e., to the (—) cross section in Fig. 2(a)]. We can virtually follow the rotation process as a function of external field by the gradual peak shift towards the saturation position [Fig. 3(a) and Fig. 4(a)] because NSF cross sections are only sensitive

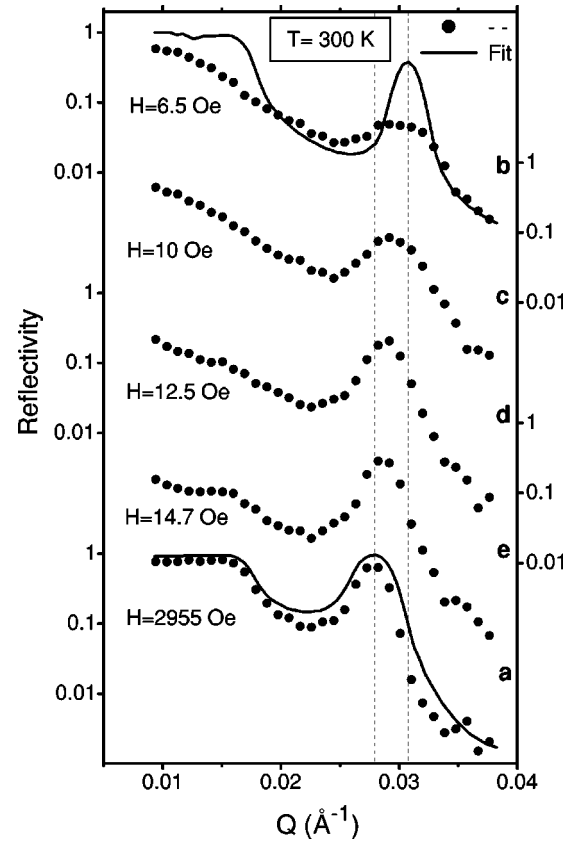


FIG. 4. Same as Fig. 3 for the unbiased state ( $T=300$  K).

on the projection of the magnetization in the field direction. The behavior is almost identical in both cases. Thus, in the unbiased state ( $T=300$  K) magnetization reversal is mainly due to rotation on both sides of the hysteresis loop whereas in the biased state ( $T=10$  K) rotation is the dominant mechanism only for increasing fields. For decreasing fields which are in the direction opposite the bias (antiparallel to  $H_{cool}$ ), the mechanism changes to a reversal which is due to DW motion. That is, in the biased state the antiferromagnet strongly affects the reversal of the ferromagnet in the direction opposite the bias whereas for the return into the bias direction the antiferromagnet obviously does not have any significant effect. The origin of the change in magnetization reversal is most likely connected with the strongly unidirectional character of EB coupling for the present multilayer. An appreciable energy barrier for reversal may be provided only opposite the bias direction probably due to formation of a DW in the antiferromagnet.<sup>8,9,21–24</sup>

Recent investigations have shown that depending on the particular system DW motion and rotation can both play a major role for the reversal.<sup>8–12,15,16</sup> In some of the cases where soft magnetic NiFe alloys are used as FM material and FeMn alloys as AFM material, DW motion occurs on both sides of the hysteresis loop.<sup>8,9,15</sup> For a wedge-shaped NiFe/FeMn bilayer, an asymmetry of the DW motion for increasing and decreasing fields has been found. This has also been attributed to the formation of a DW in the antiferromagnet.<sup>9</sup> The situation is more complicated for complex microstructures of the antiferromagnet such as in  $MnF_2/Fe$  and

FeF<sub>2</sub>/Fe bilayers.<sup>10,12</sup> An asymmetry in the reversal has been revealed only for a certain cooling field orientation: rotation for decreasing fields and DW motion for increasing fields. The observed orientation dependence and the type of reversal have been explained by an effective “45° coupling” which is caused by a twinned nature of the antiferromagnet. The tendency of the unidirectional anisotropy to align the magnetization with the bias direction has been assumed to favor DW motion rather than rotation only for increasing fields. We definitely find rotation as the dominant mechanism in the increasing field branch. The reason for this discrepancy is most likely due to different properties of the used AFM materials. Extremely different film thicknesses of 50 nm for MnF<sub>2</sub> and of only 2 nm for CoO may strongly influence DW formation in the antiferromagnet. More importantly, the strength of EB and the type of reversal do not significantly depend on the cooling field orientation in the case of CoO. It should also be noted that reversal asymmetry for MnF<sub>2</sub>/Fe has been found for a cooling field orientation

corresponding to a weak EB effect ( $H_E = -30$  Oe,  $E_{int} \approx 0.06$  erg/cm<sup>2</sup>, and  $H_E/H_C = 0.20$ ). The present results emphasize the necessity to clearly distinguish between different groups of systems both experimentally and theoretically even if asymmetry in EB systems is pervasive.

In summary, we have found a drastic change in the magnetization reversal processes in a [Co/CoO/Au]<sub>20</sub> multilayer. For the unbiased state ( $T = 300$  K), reversal is due to rotation on both sides of the hysteresis loop. For the biased state ( $T = 10$  K), rotation is the main mechanism only for increasing fields. For the decreasing field branch, which is the direction opposite the bias (cooling field), the mechanism changes to DW motion. That is, for the EB state the antiferromagnet affects the reversal of the ferromagnet only in the direction opposite to the bias whereas for the transition back into the bias the antiferromagnet appears not to have any significant effect. A drastic change of magnetic behavior observed exclusively opposite the pinning direction is most naturally expected for a system with strong unidirectional anisotropy.

- 
- <sup>1</sup>W. H. Meiklejohn and C. B. Bean, *Phys. Rev.* **105**, 904 (1957).  
<sup>2</sup>J. Nogués and I. K. Schuller, *J. Magn. Magn. Mater.* **192**, 203 (1999).  
<sup>3</sup>C. Tsang and K. Lee, *J. Appl. Phys.* **53**, 2605 (1982).  
<sup>4</sup>C. A. Kleint, M. K. Krause, R. Höhne, T. Walter, H. C. Semmelhack, M. Lorenz, and P. Esquinazi, *J. Appl. Phys.* **84**, 5097 (1998).  
<sup>5</sup>J. Nogués, T. J. Moran, D. Lederman, Ivan K. Schuller, and K. V. Rao, *Phys. Rev. B* **59**, 6984 (1999).  
<sup>6</sup>H. Xi and R. M. White, *J. Appl. Phys.* **87**, 410 (2000).  
<sup>7</sup>M. Gruyters and D. Riegel, *J. Appl. Phys.* **88**, 6610 (2000).  
<sup>8</sup>V. I. Nikitenko, V. S. Gornakov, L. M. Dedukh, Yu. P. Kabanov, A. F. Khapikov, A. J. Shapiro, R. D. Shull, A. Chaiken, and R. P. Michel, *Phys. Rev. B* **57**, R8111 (1998).  
<sup>9</sup>V. I. Nikitenko, V. S. Gornakov, A. J. Shapiro, R. D. Shull, Kai Liu, S. M. Zhou, and C. L. Chien, *Phys. Rev. Lett.* **84**, 765 (2000).  
<sup>10</sup>M. R. Fitzsimmons, P. Yashar, C. Leighton, Ivan K. Schuller, J. Nogués, C. F. Majkrzak, and J. A. Dura, *Phys. Rev. Lett.* **84**, 3986 (2000).  
<sup>11</sup>X. Portier, A. K. Petford-Long, A. de Morais, N. W. Owen, H. Laidler, and K. O’Grady, *J. Appl. Phys.* **87**, 6412 (2000).  
<sup>12</sup>C. Leighton, M. R. Fitzsimmons, P. Yashar, A. Hoffmann, J. Nogués, J. Dura, C. F. Majkrzak, and Ivan K. Schuller, *Phys. Rev. Lett.* **86**, 4394 (2001).  
<sup>13</sup>S. Methfessel, S. Middlehoek, and H. Thomas, *J. Appl. Phys.* **32**, 1959 (1961).  
<sup>14</sup>A. Khapikov, L. Uspenskaya, J. Ebothe, and S. Vilain, *Phys. Rev. B* **57**, 14 990 (1998).  
<sup>15</sup>O. Bostanjoglo and P. Kreisel, *Phys. Status Solidi A* **7**, 173 (1971).  
<sup>16</sup>H. D. Chopra, David X. Yang, P. J. Chen, H. J. Brown, L. J. Swartzendruber, and W. F. Egelhoff, Jr., *Phys. Rev. B* **61**, 15 312 (2000).  
<sup>17</sup>M. Gruyters and D. Riegel, *Phys. Rev. B* **63**, 052401 (2001).  
<sup>18</sup>F. Mezei, R. Golub, F. Klose, and H. Toews, *Physica B* **213-214**, 898 (1995).  
<sup>19</sup>L. G. Parratt, *Phys. Rev.* **95**, 359 (1954); the software used, PARRATT32, was developed by C. Braun for Hahn-Meitner-Institut Berlin.  
<sup>20</sup>S. G. E. te Velthuis, A. Berger, G. P. Felcher, B. K. Hill, and E. Dan Dahlberg, *J. Appl. Phys.* **87**, 5046 (2000).  
<sup>21</sup>D. Mauri, H. C. Siegmann, P. S. Bagus, and E. Kay, *J. Appl. Phys.* **62**, 3047 (1987).  
<sup>22</sup>A. P. Malozemoff, *Phys. Rev. B* **35**, 3679 (1987).  
<sup>23</sup>M. D. Stiles and R. D. McMichael, *Phys. Rev. B* **59**, 3722 (1999).  
<sup>24</sup>J. Geshev, *Phys. Rev. B* **62**, 5627 (2000).